



PCCP

**AFIR explorations of transition states of extended unsaturated systems: automatic location of ambimodal transition states**

Journal:	<i>Physical Chemistry Chemical Physics</i>
Manuscript ID	CP-ART-05-2020-002379.R1
Article Type:	Paper
Date Submitted by the Author:	04-Jun-2020
Complete List of Authors:	Ito, Takuma ; Graduate School of Chemical Sciences and Engineering, Hokkaido University Harabuchi, Yu; Hokkaido University, Department of Chemistry, Faculty of Science; JST, PRESTO, Maeda, Satoshi; Faculty of Science, Hokkaido University, Chemistry

SCHOLARONE™  
Manuscripts

# AFIR explorations of transition states of extended unsaturated systems: automatic location of ambimodal transition states

Takuma Ito,<sup>a</sup> Yu Harabuchi,<sup>b,c,d,e\*</sup> and Satoshi Maeda<sup>b,c,d\*</sup>

<sup>a</sup> Graduate School of Chemical Sciences and Engineering, Hokkaido University, Sapporo 060-8628, Japan.

<sup>b</sup> Department of Chemistry, Faculty of Science, Hokkaido University, Sapporo 060-0810, Japan.

<sup>c</sup> Institute for Chemical Reaction Design and Discovery (WPI-ICReDD), Hokkaido University, Sapporo 001-0021, Japan

<sup>d</sup> JST, ERATO Maeda Artificial Intelligence for Chemical Reaction Design and Discovery Project, Sapporo 060-0810, Japan

<sup>e</sup> JST, PRESTO, 4-1-8 Honcho, Kawaguchi, Saitama, 332-0012, Japan

**Corresponding authors:** Yu Harabuchi ([y\\_harabuchi@sci.hokudai.ac.jp](mailto:y_harabuchi@sci.hokudai.ac.jp)), Satoshi Maeda ([smaeda@eis.hokudai.ac.jp](mailto:smaeda@eis.hokudai.ac.jp))

**Notes:** The authors declare no competing financial interest.

**Abstract:** Paths of Diels-Alder reactions between 2-vinylfuran and 3-methoxycarbonylcyclopentadienone were systematically explored by the multicomponent version of the artificial force induced reaction (MC-AFIR) method. In this reaction, the dynamical bifurcation in which a single transition state (TS) relates to two different products has been reported to occur [J. B. Thomas, et al. *J. Am. Chem. Soc.*, 2008, **130**, 14544-14555]. In this paper, based on the MC-AFIR method, we propose a procedure to systematically explore so called ambimodal TSs through which the dynamical bifurcation occurs. The present procedure finds candidates of TSs that may cause the dynamical bifurcation from the logs of automated reaction path search by the MC-AFIR method, without any additional quantum chemical calculations. For this reaction, the MC-AFIR search found 125 unique TSs automatically. Among the 125 TSs, 19 were suggested as candidates, and finally, six including the one reported in the literature were confirmed to cause the dynamical bifurcation. The present procedure would be promising to find TSs involved in the dynamical bifurcation automatically.

**keywords (up to five keywords)**

Reaction path, dynamical bifurcation, potential energy surface, reaction mechanism, DFT calculation

## I. Introduction

The Diels-Alder reaction is one of the most important synthesis methods and has been utilized in vast chemical syntheses.<sup>1,2</sup> Its transition state (TS) has also been studied extensively based on quantum chemical calculations.<sup>3</sup> On the other hand, several groups have reported Diels-Alder reactions in which a phenomenon so-called dynamical bifurcation takes place.<sup>4,5</sup> The dynamical bifurcation in the Diels-Alder reaction is the focus of this paper.

Theoretically, an elementary reaction step is defined as a path that connects a pair of two local minima via a single transition state (TS). These paths are commonly defined by the steepest descent path starting from a TS in the mass-weighted coordinates and called intrinsic reaction coordinate (IRC).<sup>6,7</sup> By calculating an IRC path, energetic and geometrical variations that occur in the corresponding reaction step can be elucidated.

In most reactions, the IRC path well represents the mechanism of corresponding reaction. However, actual molecular motions deviate from the IRC path due to the kinetic energy, and there are known cases where the neglect of kinetic energy misleads an incorrect mechanism.<sup>8-10</sup> The dynamical bifurcation is one of such cases.<sup>11-28</sup> In a bifurcation reaction, a single TS relates to two products. In other words, a set of reactive trajectories passing the corresponding TS region branches into two components giving two different products. Such a TS is called an ambimodal TS.<sup>5</sup> Since an IRC calculation from a TS gives only a single product, the IRC calculation misses one of two products in bifurcation reactions.<sup>29</sup>

Occurrence of bifurcation can be recognized by running *ab initio* molecular dynamics (AIMD) simulations starting from the corresponding TS region.<sup>30-53</sup> Therefore, AIMD simulations have been performed to reveal bifurcations in reactions of various types such as organic reactions,<sup>30-35,37,38,43-45,47,49-57</sup> organometallic reactions,<sup>41,58</sup> and biosynthesis reactions.<sup>36,39,59-64</sup> Occurrence of bifurcation can also be discussed through a static analysis of the potential energy surface (PES) by locating a valley-ridge transition (VRT) point along the IRC path. On a VRT point, the shape of PES perpendicular to the IRC path changes from the valley to the ridge.<sup>11,12,15,16,20,21,23,24,26,27</sup> To find a VRT point, the curvature of PES needs to be computed at many points along the IRC path.

Our purpose in this paper is to systematically explore TSs from which a dynamical bifurcation takes place. In the pioneering work by Hong and Tantillo,<sup>64</sup> they applied AIMD simulations to various TSs in a reaction path network of terpene and discussed bifurcation reactions on the network. To avoid running AIMD simulations from many TSs, Harabuchi et al. systematically explored VRT points by applying the curvature analysis along all IRC paths on a reaction path network of Au<sub>5</sub> cluster.<sup>65</sup> Then, they applied AIMD simulations to only TSs from which a VRT point was obtained to identify products of corresponding bifurcation reactions. Although this approach allowed them to avoid AIMD simulations from many TSs, the curvature analysis done in their VRT search needs to compute Hessian matrix and is still demanding computationally.

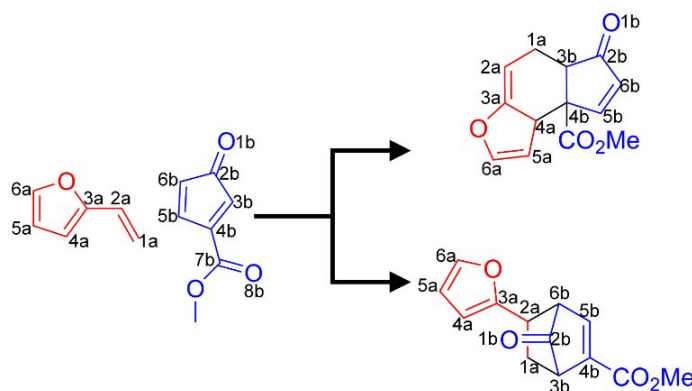
Our approach proposed here was inspired by results in early studies where two different products were obtained for the same TS depending on the choice of coordinate systems.<sup>22</sup>

Subsequent AIMD studies revealed that a dynamical bifurcation took place from the TS.<sup>50-52</sup> In this discovery, use of paths of two different mathematical nature was the key. In other words, both of the two products were identified by computing two static paths with different mathematical nature. We have developed an automated reaction path search method called artificial force induced reaction (AFIR).<sup>66,67</sup> The AFIR method traces a path so-called AFIR path because AFIR paths can be computed easily from a local minimum to the other local minimum. In the standard AFIR procedure, all obtained AFIR paths are further processed to obtain actual TSs. Therefore, our idea here is that two bifurcation products could be identified from differences between connections of AFIR paths and IRC paths. It is thus expected that this approach could suggest both occurrence and products of bifurcation reactions without any additional efforts after an automated reaction path search.

In this study, we explored paths of reactions between 2-vinylfuran and 3-methoxycarbonylcyclopentadienone (see **scheme 1**) systematically by the multicomponent version of the AFIR method (MC-AFIR).<sup>66</sup> These two reactants are known to react to each other affording two Diels-Alder products. Furthermore, paths leading these two products are known to share a single TS and thus correspond to a bifurcation reaction. Moreover, this system has many reactive sites at which different competing Diels-Alder reactions can take place. Actually, the MC-AFIR search generated paths to sixty-five unique products, where these products were unique in terms of their SMILES representation. Among the sixty-five, sixteen corresponded to Diels-Alder products. As expected, we found many cases in which the reactants were linked to a product via

only an AFIR path. In these cases, through a careful analysis of search logs of obtaining actual TSs, it was found that two AFIR paths shared a single TS region as the bottleneck. The further curvature analysis of IRC paths from these TSs identified six cases in which VRT points existed along the corresponding IRC paths. Finally, we proposed six bifurcation cases for this single reaction system.

**Scheme 1.** Diels-Alder cycloaddition reaction<sup>33</sup> between 2-vinylfuran and 3-methoxycarbonylcyclopentadienone.



## II. Theory

The AFIR method induces a structural deformation in a system by an artificial force and finds a path of chemical reaction from a local minimum to the other local minimum. The structural deformation can be induced by minimizing a function so-called AFIR function.<sup>66</sup> Thanks to careful design of the form of AFIR function, paths that are obtained through its minimization pass TS regions that actual reaction paths pass.<sup>66,68</sup> Therefore, the AFIR method first explores AFIR paths and finds TSs for various reactions by further processing the AFIR paths. Details how it

systematically explores AFIR paths and how actual TSs are obtained from AFIR paths are described in our previous papers.<sup>66-69</sup>

Our idea or hypothesis proposed in this study is explained using a 2-dimensional model PES shown in **Figure 1**. On this PES, three local minima, **R**, **P1**, and **P2**, and two TSs, **T1** and **T2**, exist. Let's consider the process of finding paths to **P1** and **P2** by the AFIR method starting from **R**. In this case, the AFIR method finds these two products by adding artificial forces along different directions. The corresponding AFIR paths are depicted as white lines. These AFIR paths pass the **T1** region, and further geometry optimizations starting from the highest energy points along these AFIR paths converge to **T1**. In the actual application to the molecular system shown below, an additional procedure of relaxing the AFIR path was taken to avoid failure of TS optimization (see the computational details section for more description). Finally, the IRC path is computed from **T1**. The IRC path from **T1** toward products' valley once approaches to **T2** and finally falls into **P1**'s well.



useful when the mechanism of the target reaction is unknown. In such a case, the automated search by the AFIR method is effective because the search systematically finds possible paths and help identifying the most probable mechanism. After the search, one can reveal both occurrence and products of possible dynamical bifurcations just by analyzing search logs without any additional quantum chemical calculations.

### III. Results and Discussion

The Diels-Alder cycloaddition is a [4+2] cycloaddition reaction between a conjugated diene and dienophile. In this study, a case between 2-vinylfuran and 3-methoxycarbonylcyclopentadienone is studied (see **scheme 1**). For this reaction, occurrence of a bifurcation was previously reported.<sup>33</sup> The reported bifurcation for this reaction gave two Diels-Alder products; one is the cycloaddition product composed of C3b, C4b, C5b, and C6b in cyclopentadienone and C1a and C2a in 2-vinylfuran (denoted by [C3b-C6b+C1a-C2a] type), and the other is that of C3b and C4b in cyclopentadienone and C1a, C2a, C3a, and C4a in 2-vinylfuran (denoted by [C1a-C4a+C3b-C4b] type). In other words, a cyclopentadienone acts as diene in the case of [C3b-C6b+C1a-C2a] type, while 2-vinylfuran acts as diene in the case of [C1a-C4a+C3b-C4b] type. This type of bifurcation was called a bispericyclic reaction.<sup>4</sup> Thus, fragment-A was set to C3b, C4b, C5b, and C6b in cyclopentadienone, and fragment-B is set to as C1a, C2a, C3a, and C4a in 2-vinylfuran.

The systematic AFIR search generated 134 product-MINs and 125 TSs automatically. The

search found not only paths of [4+2] cycloaddition but also those of the other types such as [2+2] cycloaddition, [4+4] cycloaddition, [6+2] cycloaddition, and [6+4] cycloaddition. The obtained TSs are ordered in the ascending order of their energies and termed TS $x$  ( $x = 0 \sim 124$ ), where all energy values below are relative to the total energy of reactants. The lowest TS $0$  is for the [4+2] cycloaddition in **Scheme 1**. It was found that two AFIR paths shared TS $0$ . These two AFIR paths lead to [C1a-C4a+C3b-C4b] and [C3b-C6b+C1a-C2a] products, respectively. This suggests that TS $0$  serves as a TS of bifurcation giving [C1a-C4a+C3b-C4b] and [C3b-C6b+C1a-C2a] products. This is consistent with the previous discovery summarized in **scheme 1**.<sup>33</sup>

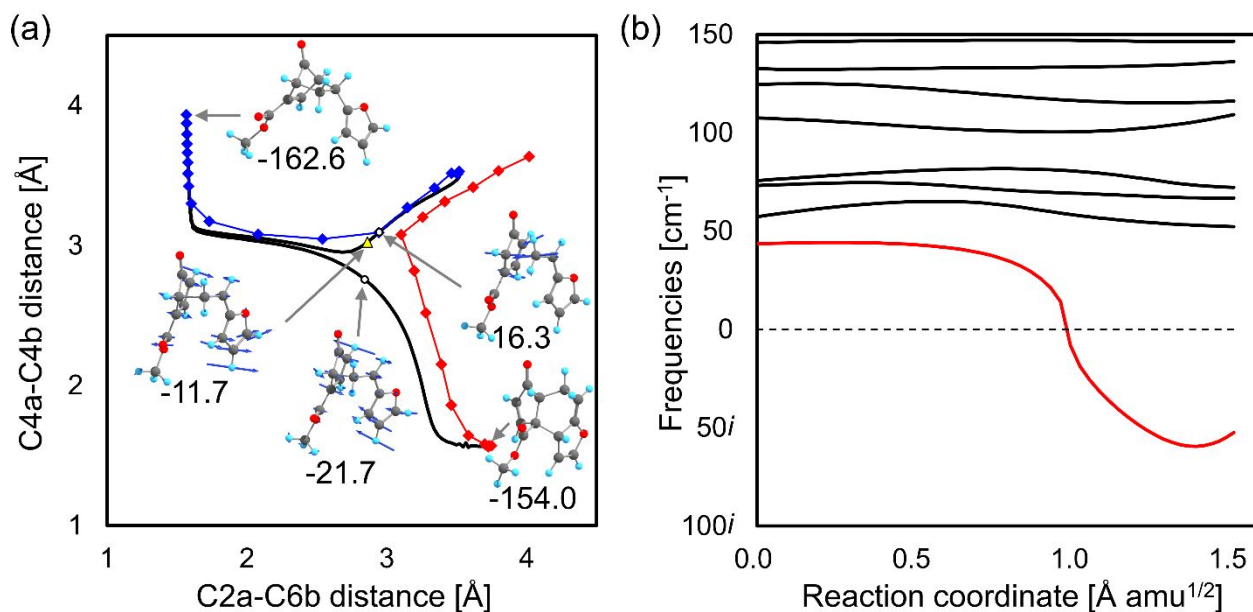


**Figure 2.** Analyses of AFIR paths and IRC paths. (a) shows a plot for C2a-C6b distance ( $x$ -axis) versus C4a-C4b distance ( $y$ -axis) along the IRC paths and the AFIR paths. Blue and red lines indicate AFIR paths, black lines indicate IRC paths, circles indicate TSs, and a triangle indicates a VRT point. Structures of TSs, MINs, and a VRT point are shown. Normal mode vectors corresponding to the negative eigenvalue mode at TSs and a VRT point are depicted. (b) shows the eight lowest vibrational frequencies of the modes perpendicular to the product side of the IRC path from  $s = 0.0 \text{ \AA}$  to  $1.5 \text{ \AA}$  for TS0. Red line corresponds to the mode related to the dynamical bifurcation. All electronic energies are shown in  $\text{kJ mol}^{-1}$  relative to the set of reactants.

**Figure 2a** compares variations of two internal coordinates along the IRC path from TS0 with those along the two AFIR paths, where the AFIR paths shown in this figure were obtained by relaxing the initial AFIR paths of the low computational level by the final computational level (see computational details). Like the two-dimensional model shown in **Figure 1**, the AFIR method

found these two products. The corresponding AFIR paths depicted as blue and red lines passed the TS region, and further geometry optimizations starting from the highest energy points along these AFIR paths converged to the TS. The IRC path computed from the TS toward products' valley once approached to the TS between the two products and finally fell into the [C1a-C4a+C3b-C4b] product.

The VRT took place along this IRC path. **Figure 2b** shows variation of the eight lowest vibrational frequencies of the modes perpendicular to the IRC path from  $s = 0.0 \text{ \AA}$  to  $1.5 \text{ \AA}$ . The negative eigenvalue mode (the red line) at the VRT point (see **Figure 2a**) is nearly parallel to the negative eigenvalue mode of the TS between the two products (see **Figure 2a**) and thus is related to the bifurcation. These results supported our idea shown in **Figure 1** and stimulated us to further study the other paths with the same idea.

Next, let's consider all [4+2] cycloaddition reactions that are assumable to occur between the diene and dienophile. There are eight combinations of diene and dienophile for [4+2] cycloaddition reactions; [C3b-C6b+C4a-C3a], [C3b-C6b+C3a-C4a], [C1a-C4a+C3b-C4b], [C1a-C4a+C4b-C3b], [C3b-C6b+C1a-C2a], [C3b-C6b+C2a-C1a], [C1a-C4a+C5b-C6b], [C1a-C4a+C6b-C5b]. All the eight patterns have endo-exo types, and thus, 16 unique [4+2] cycloadditions are expected in this system. These 16 patterns are listed in **Table 1**. As shown in **Figure 3a** and **3b**, when two dienes approach together during a Diels-Alder cycloaddition, both of [4+2] and [2+4] cycloadditions are expected. This is because both two dienes can act as the dienophile of the reaction. In this case, the [4+2] and [2+4] cycloadditions sometimes pass through



15 <sup>d</sup>	C1a-C4a	C6b-C5b	endo	24.5	TS 3	C3b-C6b	C2a-C1a	24.5	TS 3	N/A	N/A	N/A	N/A
16	C1a-C4a	C6b-C5b	exo	63.7	TS 31	N/A	N/A	N/A	N/A	N/A	N/A	N/A	N/A

<sup>a</sup>[2+4] and [4+2] cycloadditions of entry-1 correspond to [4+2] and [2+4] cycloadditions of entry-7, respectively. <sup>b</sup>[2+4] and [4+2] cycloadditions of entry-3 correspond to [4+2] and [2+4] cycloadditions of entry-13, respectively. <sup>c</sup>[2+4] and [4+2] cycloadditions of entry-5 correspond to [4+2] and [2+4] cycloadditions of entry-9, respectively. <sup>d</sup>[2+4] and [4+2] cycloadditions of entry-11 correspond to [4+2] and [2+4] cycloadditions of entry-15, respectively.

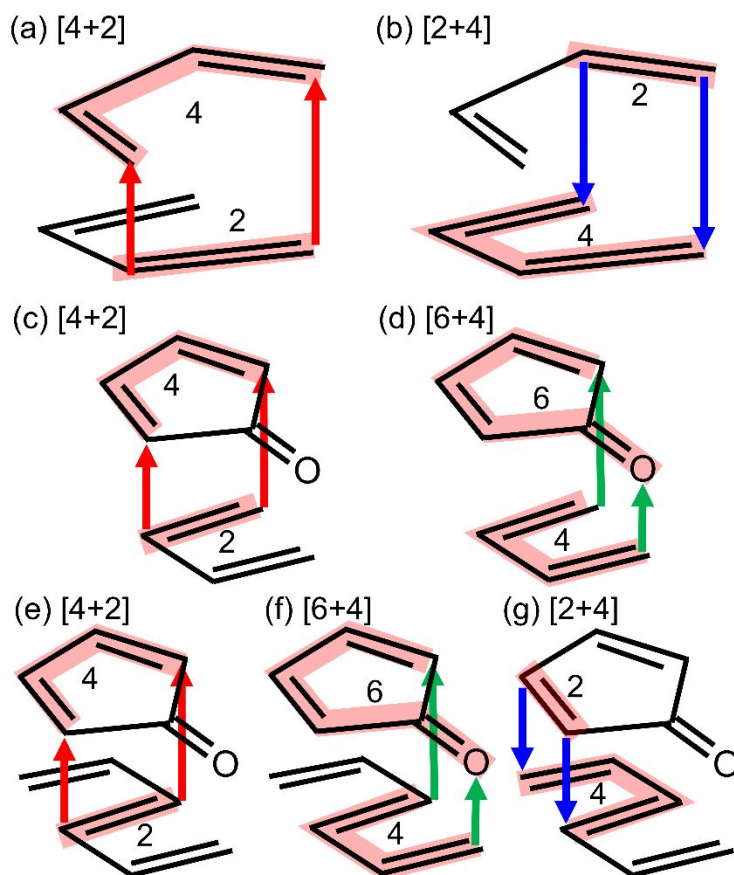


**Figure 3.** Schematic picture of bispericyclic bifurcations. (a) and (b) are for the case of [4+2]/[2+4] bispericyclic reactions. (c) and (d) are for [4+2]/[6+4] bispericyclic reactions. (e), (f) and (g) are for the case where both of [4+2]/[2+4] bispericyclic reactions or [4+2]/[6+4] bispericyclic reactions are expected.

Similarly, [4+2] and [6+4] cycloadditions sometimes pass through a common TS geometry, when a diene and a triene parts approach together during a [4+2] Diels-Alder cycloaddition like **Figure 3c** and **3d**. This type is indicated by a [4+2]/[6+4] bispericyclic reaction,

and the expected [6+4] reactions are indicated in **Table 1**. In the four cases, i.e. entry-1, 2, 3, 4, 10 and 12, there were possibilities of [4+2]/[6+4] bispericyclic reaction. On the other hand, there was no candidate expected for the other eight cases, because a diene in 2-vinylfuran does not approach triene in cyclopentadienone during the reaction of eight cases, which are indicated by N/A in **Table 1**. Actually, all the expected [6+4] products were also obtained by the present AFIR search.

In the results of the present search, a common TS region was shared by two AFIR paths in seven cases among the 16 bispericyclic reactions listed in **Table 1**. All the seven cases are indicated by a black flame in **Figure 4**. Entry-3, 10 and 12 correspond to [4+2]/[6+4] bispericyclic reactions, and entry-5 (equal to entry-9), 6, 8, and 11 (equal to entry-15) correspond to [4+2]/[2+4] bispericyclic reactions. On the other hand, two different TSs were found for a pair of AFIR paths for [4+2]/[6+4] bispericyclic pair of entry-1,2, and 4, and for [4+2]/[2+4] bispericyclic pair of entry-1,2,3 and 4. In the case of entry-3, [4+2]/[2+4] bispericyclic pair was not found, although that of [4+2]/[6+4] was found. This is explained by the absence of a common chemical bond generated during cycloaddition reactions. As shown in **Figure 3e, 3f, and 3g**, a common chemical bond is generated during [4+2] and [2+4] cycloadditions, and the situation is same for [4+2] and [6+4] cycloadditions. However, there is no common chemical bond generated during [2+4] and [6+4] cycloadditions, which makes their TSs different. In the cases of entry-1, 2, and 4, three AFIR path had the own TSs. This is explained based on the energy on TSs which connect two product minima. When a bifurcation occurs along a path from reactant-1 (denoted by R1) to product-1 (denoted by P1) and product-2 (denoted by P2), the TS connecting R1 to P1/P2 must be higher than the TS

connecting P1 and P2. This is because a dynamical bifurcation leading to P1 and P2 takes place along a decent path from TS between R1 and P1/P2. In other words, a dynamical bifurcation does not occur when the TS between P1 and P2 is higher than the TS between R1 and P1/P2. In the three cases of entry-1, 2, and 3, the TSs between products were higher than the lowest TS which connected the reactant and product. Thus, these are not cases of dynamical bifurcations. In short, there were the seven cases among the 16 bispericyclic reactions where the TS between P1 and P2 was lower than the TS between R1 to P1/P2, and, in the all the seven cases, a common TS region was shared by two AFIR paths.

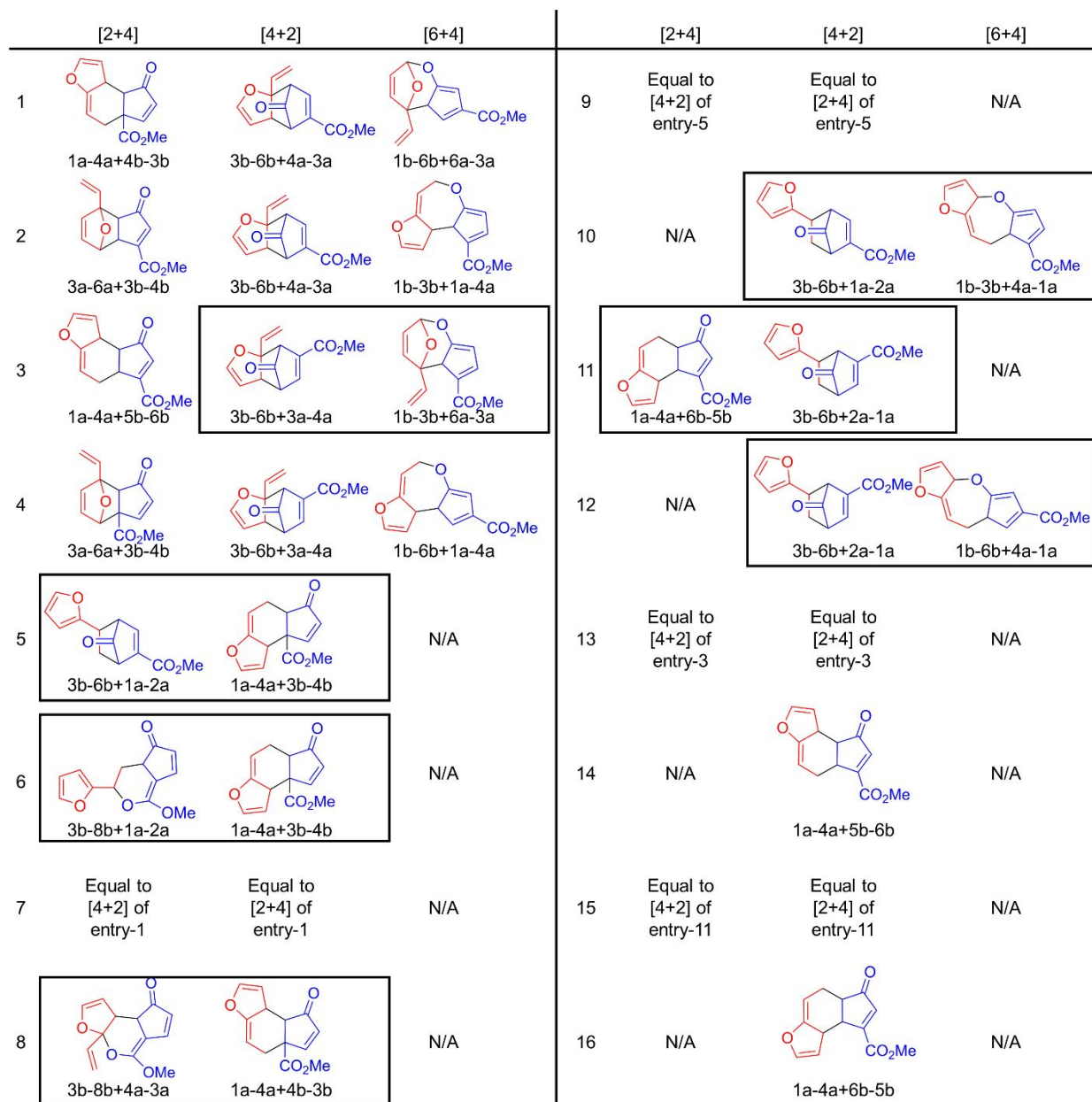


**Figure 4.** Expected [4+2] cycloaddition products for the target reaction. All the 16 [4+2] cycloaddition (Diels-Alder) products indicated in **Table 1** are shown. The obtained [2+4] and [6+4] cycloaddition products which can be paired with [4+2] cycloadditions as bispericyclic reactions are indicated in the corresponding row. Black frames indicate the cases where two AFIR paths to the products shared a common TS. “N/A” indicates a not-applicable case.

Finally, all the obtained AFIR paths and TSs are summarized. In **Figure 5**, energies of all

the obtained TSs in the search, i.e. 125 TSs, were plotted against the indices of atom pairs for each TS. Here,  $i$ - $j$  indicates the atom pair with the shortest atom-atom distance between the two reactants on each TS. Red and green dashed line indicates a TS shared by two or more AFIR paths which gave products with different SMILES representations, and blue dotted line indicates that for the same SMILES representations. Black solid line indicates a TS for one AFIR path. Red dashed lines are for the cases when the VRT corresponding to the bifurcation was found along the IRC path, and green dashed line are for these without the VRT. All the structures for the obtained TSs are shown in the supporting information

Interestingly, there were 29 cases where a common TS was shared by two AFIR paths, and there were six cases where a common TS was shared by three AFIR paths. The latter case is related to a trifurcation reported in a previous study.<sup>28</sup> Thus, totally 35 candidates of bifurcations were found in the present search. In 16 cases among the 35 cases, two different product minima had the same SMILES representations, which corresponds to the reactions giving conformationally different products. In 19 cases among the 35 cases, two different product minima had different bonding patterns. Among these 19 cases, there was the VRT corresponding to the bifurcation along the IRC path in six cases (indicated by red dashed lines in **Figure 5**). The TS geometries and the products of the six cases were depicted in ascending order of TS energies in **Figure 6**.

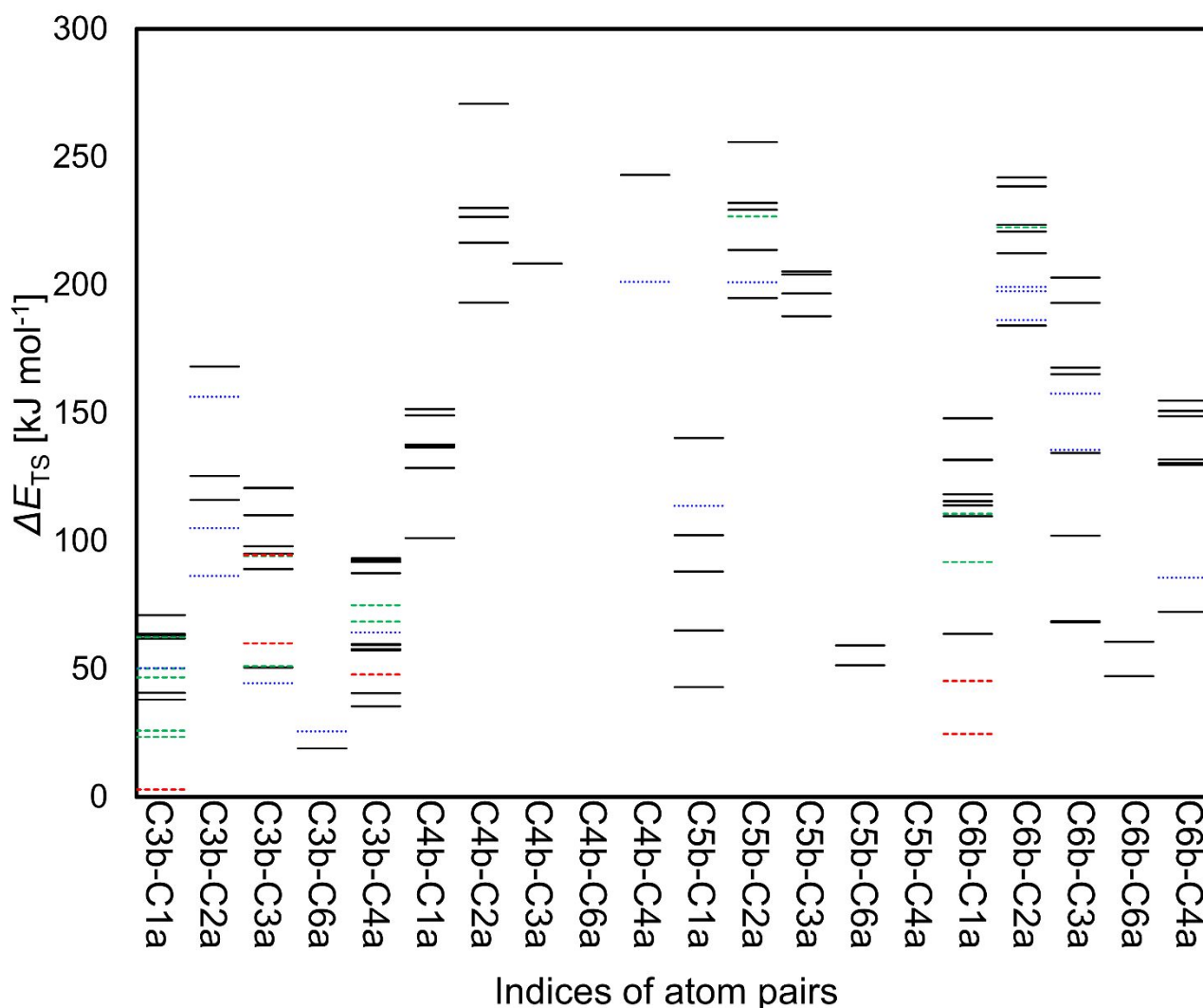


**Figure 5.** A plot of  $\Delta E_{\text{TS}}$  against indices of the closest atom pairs on TSs. Black solid lines indicate TSs that one AFIR path passes through it. Blue dotted lines indicate TSs shared by two or more AFIR paths which gave products with the same SMILES representations. Green and red dashed lines indicate TSs shared by two or more AFIR paths which gave products with different SMILES representations. Red dashed lines indicate TSs with a VRT on its IRC path, and green dashed lines indicate TSs without any VRTs.

In **Figure 6**, in addition to the [4+2]/[2+4] bispericyclic reactions and [4+2]/[6+4] bispericyclic reactions expected in **Table 1** (TS0, TS3, TS12, TS15, and TS26), the other one

(TS51) was listed. The case of TS51 is a bifurcation to a [2+2] product and a [4+4] product, which has not been known previously. It is emphasized that the prediction of this bifurcation is not easy, but it was automatically obtained by using the present approach without using any prior knowledges of the reaction. These results demonstrate usefulness of the present approach to search for bifurcations.

As shown in **Figure 6**, for all the six cases, the TS energies,  $\Delta E_{\text{TS}}$ , was lower than 110 kJ mol<sup>-1</sup>. Also, the six cases correspond to the reaction in which the atom pair was composed by the terminal carbon atoms of a diene, C3b or C6b of cyclopentadienone, and C1a, C3a, C4a, or C6a of 2-vinylfuran. Thus, it is concluded that, in this system, the bifurcations accompany the bond formation between the terminal carbon atoms of the dienes.

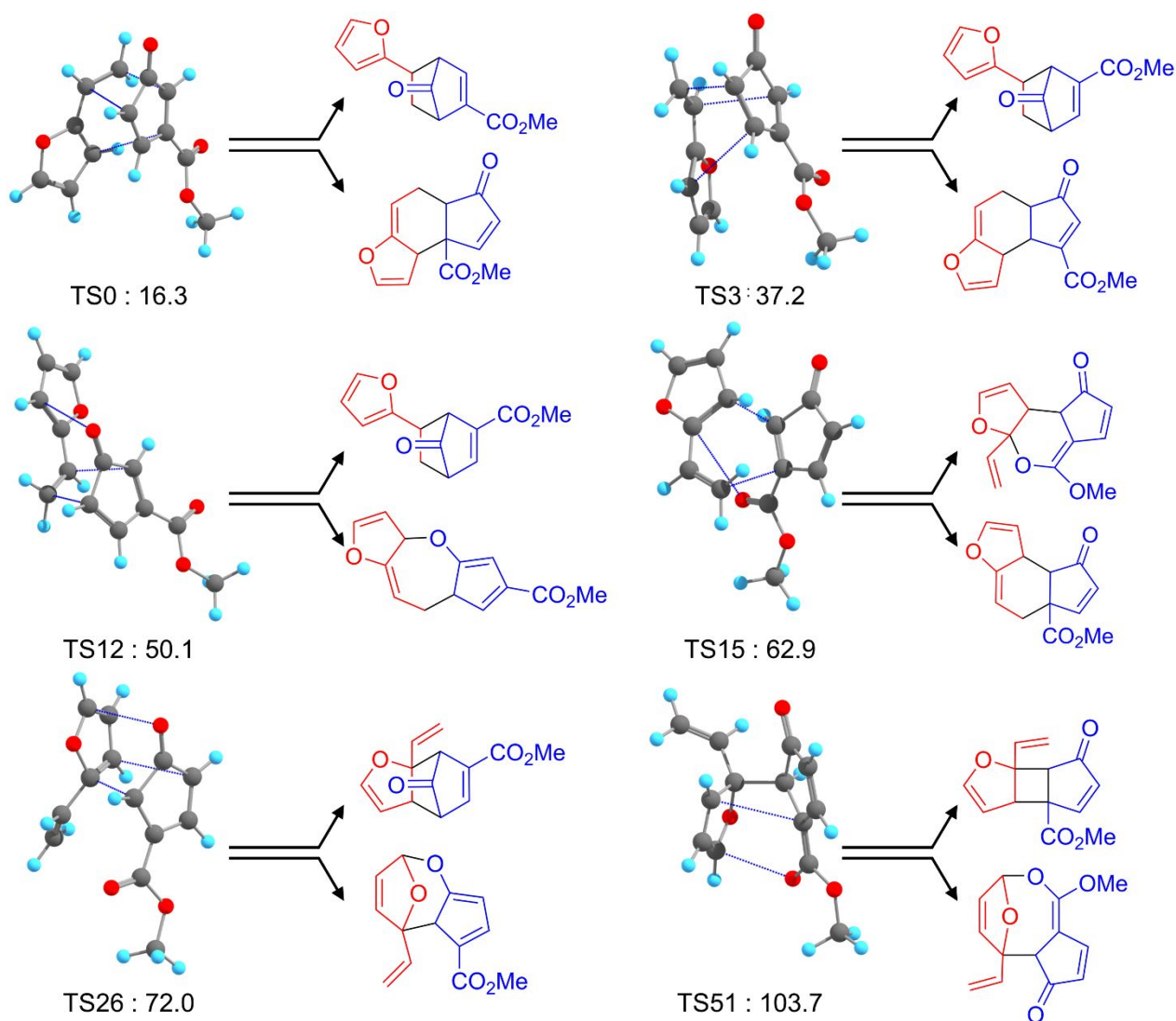


**Figure 6.** Six cases in which a common TS region was shared by two AFIR paths to reach two different product minima with different SMILES representations. In all the six cases, a VRT was found on the IRC path. Blue dotted line indicates the atom pair which makes the chemical bond during the reaction. TS energies are also indicated in  $\text{kJ mol}^{-1}$ .

#### IV. Conclusion

In this study, paths of Diels-Alder reactions between 2-vinylfuran and 3-methoxycarbonylcyclopentadienone were systematically explored by the MC-AFIR method. This reaction is known to give two Diels-Alder products from a single TS region through the dynamical

bifurcation.<sup>33</sup> In this study, we proposed a procedure to systematically predict cases in which the dynamical bifurcation occurs and applied it to the reaction. In this procedure, occurrence of the dynamical bifurcation is identified by collecting cases where AFIR paths to different products share a single TS region. The idea was inspired by an early study in which steepest descent paths computed in different coordinate systems led two different products of the dynamical bifurcation.<sup>22</sup>

The present MC-AFIR search generated 125 TSs to 65 unique products. In addition to all possible [4+2] cycloaddition paths (Diels-Alder reactions), paths of the other cycloaddition types such as [2+2] cycloaddition, [4+4] cycloaddition, [6+2] cycloaddition, and [6+4] cycloaddition were also found. In 19 among all the 125 TSs, two AFIR paths shared a single TS region as the bottleneck and gave product minima different in terms of SMILES representation. Then, these 19 cases were further studied, and in 6 cases among the 19, a VRT point was found along the corresponding IRC path. Therefore, these six including the one reported in the literature<sup>33</sup> were proposed as TSs causing the dynamical bifurcation. The five new cases corresponded to two [4+2]/[2+4] bispericyclic reactions, two [4+2]/[6+4] bispericyclic reactions, and the other. The present procedure can find TSs causing dynamical bifurcations without using any prior knowledge on the target reaction and thus would be promising in future mechanistic studies on reactions involving dynamical bifurcations.

## V. Computational Details

The AFIR paths between fragments A and B were computed starting from 1500 random

mutual positions and orientations between 2-vinylfuran and 3-methoxycarbonylcyclopentadienone. The maximum model collision energy parameter,  $\gamma$ , was set to 1000 kJ mol<sup>-1</sup>. The obtained AFIR paths were reoptimized using the LUP method,<sup>70</sup> and the energy maxima along the LUP paths were optimized to the actual TSs. From all obtained TSs, the IRC path was computed. These calculations were done at the  $\omega$ B97X-D<sup>71</sup>/D95V level. AFIR paths passing the TS0 region were further relaxed by the LUP method at the MPW1K/6-31+G\*\* level to compare the results with those in the literature.<sup>33</sup> 19 TSs which were shared by two AFIR paths giving products different in terms of SMILES representation were further optimized at the MPW1K/6-31+G\*\* level. The IRC path was calculated for these 19 TSs at the MPW1K/6-31+G\*\* level, and existence of a VRT point along the IRC path was examined through the curvature analysis using Hessian from which components along the gradient vector were eliminated.<sup>15</sup> Energy, gradient, and Hessian were computed using the Gaussian 16 program package.<sup>72</sup> AFIR, LUP, and IRC calculations were done using the developmental version of GRRM program.<sup>73</sup> In this study, a post-processing code which automatically identifies candidates of ambimodal TSs was developed independently to the GRRM program; the code is executed in the directory in which GRRM outputs exist and finds the candidates from the GRRM outputs.

### Supporting information

(I) Cartesian coordinates of the optimized TS structures at the  $\omega$ B97X-D /D95V level and (II) variations in the four lowest transverse vibrational mode frequencies along the product side of the

IRC path for the TSs which are shared by two AFIR paths.

## Acknowledgements

TI is grateful to the Institute for Quantum Chemical Exploration for the IQCE fellowships for Young Scientists. This study is supported by JST-ERATO with grant number JPMJER1903. SM is supported by JST, CREST with grant number JPMJCR14L5. YH is supported by JST, PRESTO with grant number JPMJPR16N8. We thank Ms. Takako Homma for editing a draft of this manuscript.

## Reference

1. O. Diels, K. Alder, *Justus Liebigs Ann. Chem.*, 1928, **460**, 98-122.
2. K. C. Nicolaou, S. A. Snyder, T. Montagnon, G. Vassilikogiannakis, *Angew. Chem. Int. Ed.*, 2002, **41**, 1668–1698.
3. D. H. Ess, G. O. Jones, K. N. Houk, *Adv. Synth. Catal.*, 2006, **348**, 2337-2361.
4. P. Caramella, P. Quadrelli, L. Toma, *J. Am. Chem. Soc.*, 2002, **124**, 1130-1131.
5. Z. Yang, X. Dong, Y. Yu, P. Yu, Y. Li, C. Jamieson, K. N. Houk, *J. Am. Chem. Soc.*, 2018, **140**, 3061–3067.
6. K. Fukui, *Acc. Chem. Res.*, 1981, **14**, 363-368.
7. S. Maeda, Y. Harabuchi, Y. Ono, T. Taketsugu, K. Morokuma, *Int. J. Quantum Chem.*, 2015, **115**, 258 -269.
8. L. Sun, K. Song, W. L. Hase, *Science*, 2002, **296**, 875-878.

9. B. K. Carpenter, *Ann. Rev. Phys. Chem.*, 2005, **56**, 57-79.
10. D. H. Ess, S. E. Wheeler, R. G. Iafe, L. Xu, N.Çelebi-Ölçüm, K. N. Houk, *Angew. Chem. Int. Ed.*, 2008, **47**, 7592–7601.
11. A. Tachibana, I. Okazaki, M. Koizumi, K. Hori, T. Yamabe, *J. Am. Chem. Soc.*, 1985, **107**, 1190-1196.
12. P. Valtazanos, K. Ruedenberg, *Theoret. Chim. Acta.*, 1986, **69**, 281-307.
13. M. V. Basilevsky, *Theor. Chim. Acta*, 1987, **72**, 63-67.
14. W. Quapp, *Theor. Chim. Acta*, 1989, **75**, 447-460.
15. J. Baker, P. M. W. Gill, *J. Comput. Chem.*, 1988, **9**, 465-475.
16. P. Valtazanos, S. T. Elbert, S. Xantheas, K. Ruedenberg, *Theoret. Chim. Acta.*, 1991, **78**, 287-326.
17. T. Taketsugu and T. Hirano, *J. Chem. Phys.*, 1993, **99**, 9806-9814.
18. T. Taketsugu, T. Hirano, *J. Mol. Struct.: THEOCHEM*, 1994, **116**, 169-176.
19. G. N. Sastry, S. Shaik, *J. Phys. Chem.*, 1996, **100**, 12241-12252.
20. T. Taketsugu, N. Tajima, K. Hirao, *J. Chem. Phys.*, 1996, **105**, 1933-1939.
21. T. Yanai, T. Taketsugu, K. Hirao, *J. Chem. Phys.*, 1997, **107**, 1137-1146.
22. S. Shaik, D. Danovich, G. N. Sastry, P. Y. Ayala, H. B. Schlegel, *J. Am. Chem. Soc.*, 1997, **119**, 9237-9245.
23. T. Taketsugu, T. Yanai, K. Hirao, M. S. Gordon, *J. Mol. Struct.: THEOCHEM*, 1998. **451**, 163-177.

24. Y. Kumeda, T. Taketsugu, *J. Chem. Phys.*, 2000, **113**, 477-484.
25. T. Taketsugu, Y. Kumeda, *J. Chem. Phys.*, 2001, **114**, 6973-6982.
26. W. Quapp, *J. Mol. Struct.*, 2004, **695-696**, 95-101.
27. J. M. Bofill, W. Quapp, *J. Math. Chem.*, 2013, **51**, 1099-1115.
28. Y. Harabuchi, Y. Ono, S. Maeda, T. Taketsugu, K. Keipert, M. S. Gordon, *J. Comput. Chem.*, 2016, **37**, 487-493.
29. Y. Harabuchi, T. Taketsugu, *Theor. Chem. Acc.*, 2011, **130**, 305-315.
30. T. Bekele, C. F. Christian, M. A. Lipton, D. A. Singleton, *J. Am. Chem. Soc.*, 2005, **127**, 9216-9223.
31. J. Li, S. Shaik, H. B. Schlegel, *J. Phys. Chem. A*, 2006, **110**, 2801-2806.
32. B. R. Ussing, C. Hang, D. A. Singleton, *J. Am. Chem. Soc.*, 2006, **128**, 7594-7607.
33. J. B. Thomas, J. R. Waas, M. Harmata, D. A. Singleton, *J. Am. Chem. Soc.*, 2008, **130**, 14544-14555.
34. K. K. Kelly, J. S. Hirschi, D. A. Singleton, *J. Am. Chem. Soc.*, 2009, **131**, 8382-8383.
35. Z. Wang, J. S. Hirschi, and D. A. Singleton, *Angew. Chem. Int.*, 2009, **121**, 9320-9323.
36. M. R. Siebert, J. Zhang, S. V. Addepalli, D. J. Tantillo, W. L. Hase, *J. Am. Chem. Soc.*, 2011, **133**, 8335-8343.
37. X. S. Bogle, D. A. Singleton, *Org. Lett.*, 2012, **14**, 2528-2531.
38. O. M. Gonzalez-James, E. E. Kwan, D. A. Singleton, *J. Am. Chem. Soc.*, 2012, **134**, 1914-1917.

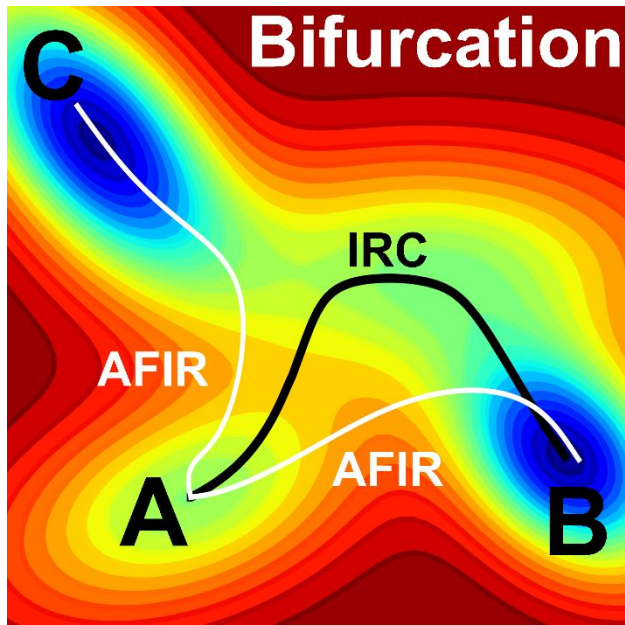
39. A. Patel, Z. Chen, Z. Yang, O. Gutiérrez, H. Liu, K. N. Houk, D. A. Singleton, *J. Am. Chem. Soc.*, 2016, **138**, 3631-3634.
40. A. Martín-Sómer, M. Yáñez, W. L. Hase, M. Gaigeot, R. Spezia, *J. Chem. Theory Comput.*, 2016, **12**, 974–982.
41. S. R. Hare, D. J. Tantillo, *Chem. Sci.*, 2017, **8**, 1442–1449.
42. S. R. Hare, R. P. Pemberton, D. J. Tantillo, *J. Am. Chem. Soc.*, 2017, **139**, 7485-7493.
43. E. L. Noey, Z. Yang, Y. Li, H. Yu, R. N. Richey, J. M. Merritt, D. P. Kjell, K. N. Houk, *J. Org. Chem.*, 2017, **82**, 5904–5909.
44. P. Yu, T. Q. Chen, Z. Yang, C. Q. He, A. Patel, Y. Lam, C. Liu, K. N. Houk, *J. Am. Chem. Soc.*, 2017, **139**, 8251-8258.
45. S. R. Hare, A. Li, D. J. Tantillo, *Chem. Sci.*, 2018, **9**, 8937–8945.
46. Z. Yang, L. Zou, Y. Yu, F. Liu, X. Dong, K. N. Houk, *Chem. Phys.*, 2018, **514**, 120–125.
47. X. Xue, C. S. Jamieson, M. Garcia-Borràs, X. Dong, Z. Yang, K. N. Houk, *J. Am. Chem. Soc.*, 2019, **141**, 1217-1221.
48. Z. Yang, C. S. Jamieson, X. Xue, M. Garcia-Borràs, T. Benton, X. Dong, F. Liu, K.N. Houk, *Tre. Chem.*, 2019, **1**, 22-34.
49. R. B. Campos, D. J. Tantillo, *Chem*, 2019, **5**, 227-236.
50. H. Yamataka, M. Aida, M. Dupuis, *Chem. Phys. Lett.*, 1999, **300**, 583-587.
51. V. Bakken, D. Danovich, S. Shaik, H. B. Schlegel, *J. Am. Chem. Soc.*, 2001, **123**, 130-134.
52. J. Li, X. Li, S. Shaik H. B. Schlegel, *J. Phys. Chem. A*, 2004, **108**, 8526-8532.

53. T. Bekele, C. F. Christian, M. A. Lipton, D. A. Singleton, *J. Am. Chem. Soc.*, 2005, **127**, 9216-9223.
54. D. A. Singleton, C. Hang, M. J. Szymanski, M. P. Meyer, A. G. Leach, K. T. Kuwata, J. S. Chen, A. Greer, C. S. Foote, K. N. Houk, *J. Am. Chem. Soc.*, 2003, **125**, 1319-1328.
55. J. Limanto, K. S. Khuong, K. N. Houk, Marc. L. Snapper, *J. Am. Chem. Soc.*, 2003, **125**, 16310-16321.
56. N.Çelebi-Ölçüm, D. H. Ess, V. Aviyente, K. N. Houk, *J. Am. Chem. Soc.*, 2007, **129**, 4528-4529.
57. H. V. Pham, K. N. Houk, *J. Org. Chem.*, 2014, **79**, 8968–8976.
58. E. L. Noey, X. Wang, K. N. Houk, *J. Org. Chem.*, 2011, **76**, 3477–3483.
59. Y. J. Hong, D. J. Tantillo, *Nat. Chem.*, 2009, **1**, 384-389.
60. Y. J. Hong, D. J. Tantillo, *Org. Biomol. Chem.*, 2010, **8**, 4589–4600.
61. D. J. Tantillo, *Nat. Prod. Rep.*, 2011, **28**, 1035–1053.
62. Y. J. Hong, S. Irmisch, S. C. Wang, S. Garms, J. Gershenson, L. Zu, T. G. Kçllner, D. J. Tantillo, *Chem. Eur. J.*, 2013, **19**, 13590 – 13600.
63. R. P. Pemberton, Y. J. Hong, D. J. Tantillo, *Pure Appl. Chem.*, 2013, **85**, 1919–2004.
64. Y. J. Hong, D. J. Tantillo, *Nat. Chem.*, 2014, **6**, 104-111.
65. Y. Harabuchi, Y. Ono, S. Maeda, T. Taketsugu, *J. Chem. Phys.*, 2015, **143**, 014301.
66. S. Maeda, K. Morokuma, *J. Chem. Phys.*, 2010, **132**, 241102.
67. S. Maeda, Y. Harabuchi, M. Takagi, T. Taketsugu, K. Morokuma, *Chem. Rec.*, 2016, **16**, 2232–

2248.

68. S. Maeda, K. Morokuma, *J. Chem. Theory Comput.* 2011, **7**, 2335–2345.
69. S. Maeda, Y. Harabuchi, M. Takagi, K. Saita, K. Suzuki, T. Ichino, Y. Sumiya, K. Sugiyama, Y. Ono, *J. Comput. Chem.*, 2018, **39**, 233–250
70. C. Choi, R. Elber, *J. Chem. Phys.*, 1991, **94**, 751.
71. J.D. Chai, M. Head-Gordon, *Phys. Chem. Chem. Phys.*, 2008, **10**, 6615-6620.
72. M. J. Frisch, G. W. Trucks, H. B. Schlegel, G. E. Scuseria, M. A. Robb, J. R. Cheeseman, G. Scalmani, V. Barone, G. A. Petersson, H. Nakatsuji, X. Li, M. Caricato, A. V. Marenich, J. Bloino, B. G. Janesko, R. Gomperts, B. Mennucci, H. P. Hratchian, J. V. Ortiz, A. F. Izmaylov, J. L. Sonnenberg, D. Williams-Young, F. Ding, F. Lipparini, F. Egidi, J. Goings, B. Peng, A. Petrone, T. Henderson, D. Ranasinghe, V. G. Zakrzewski, J. Gao, N. Rega, G. Zheng, W. Liang, M. Hada, M. Ehara, K. Toyota, R. Fukuda, J. Hasegawa, M. Ishida, T. Nakajima, Y. Honda, O. Kitao, H. Nakai, T. Vreven, K. Throssell, J. A. Montgomery, Jr., J. E. Peralta, F. Ogliaro, M. J. Bearpark, J. J. Heyd, E. N. Brothers, K. N. Kudin, V. N. Staroverov, T. A. Keith, R. Kobayashi, J. Normand, K. Raghavachari, A. P. Rendell, J. C. Burant, S. S. Iyengar, J. Tomasi, M. Cossi, J. M. Millam, M. Klene, C. Adamo, R. Cammi, J. W. Ochterski, R. L. Martin, K. Morokuma, O. Farkas, J. B. Foresman, and D. J. Fox, *Gaussian 16, Revision A.03*; Gaussian, Inc.: Wallingford, CT, 2016.
73. S. Maeda, Y. Harabuchi, Y. Sumiya, M. Takagi, M. Hatanaka, Y. Osada, T. Taketsugu, K. Morokuma, K. Ohno, GRRM, a developmental version at Hokkaido University, Sapporo,

Japan, 2020.



74.